



THE UNIVERSITY
of LIVERPOOL

Separating Crustal Gravity Signals from the Effects of the Moho

by

Charles Thomson

In partial fulfilment of the requirements for the degree of

BSc (Hons) Geophysics (Geology)

to

School of Environmental Sciences

The University of Liverpool

Student ID: 201261801

Supervisor: Leonardo Uieda

May 2020

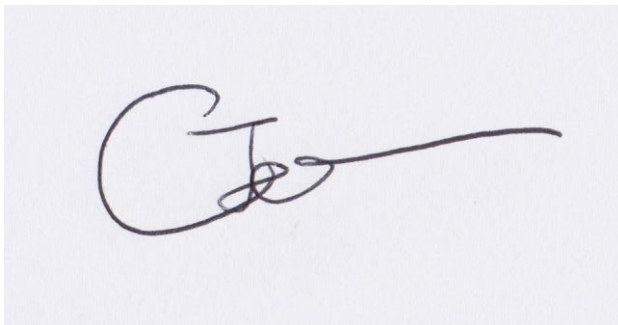
Acknowledgements

I would like to extend particular thanks to Leonardo Uieda for the continuous advice and assistance he provided during the preparation of this dissertation.

Declaration

I, Charles Thomson, confirm that the work submitted in this dissertation is my own, and that appropriate credit has been given where reference is made to the work of others.

Signature:

A handwritten signature in dark ink on a light background. The signature is stylized, starting with a large 'C' and ending with a long horizontal stroke.

Date: 04/05/2020

Table of Contents

Acknowledgements.....	ii
Declaration.....	ii
Table of Contents.....	iii
List of Figures	iv
List of Equations.....	v
Abstract.....	vi
1. Introduction	7
2. Theoretical Background	9
2.1 - Airy Isostasy	9
2.2 - Gravity/Isostasy Relationship	10
3. Methodology.....	12
3.1 - Data Acquisition	12
3.2 - Data Reduction	12
3.3 - Regression Analysis.....	14
3.4 - Robust Fit	15
3.5 - Root Mean Square	16
3.6 - Application in Windows	17
4. Results.....	18
4.1 - Regression Coefficients.....	18
4.2- Residual Values	20
4.3 - Data Misfit.....	20
4.4 - Differences between one-stage and robust two-stage regression results.....	21
4.5 - Differences between standard two-stage and robust two-stage regression results	21
5. Discussion.....	24
5.1 - Application of the regression analysis to the South Atlantic area.....	24
5.2 - Comparisons between varying regression methods	25
5.3 - Limitations	26
6. Summary	27
6.1 – Conclusion	27
6.2 - Future work.....	27
References	29

List of Figures

Figure 1 - A basic illustration of the Airy isostatic model.

Figure 2 - A basic illustration of the effect of gravity data reductions.

Figure 3 - Data profiles over the South Atlantic and confining continents.

- a) Raw gravity acquired from the EIGEN-6C4 model*
- b) The full reduced Bouguer gravity disturbance*
- c) 100km half-length Gaussian filtered topography, acquired from the ETOPO1 global relief model.*

Figure 4 - An example of the implementation of an iteratively re-weighted least-squares approach to a generic dataset.

Figure 5 – The approximated best-fit least squares solution to the Bouguer disturbance and filtered topography data over the South Atlantic.

Figure 6 – Results obtained through implementation of a robust two-stage regression analysis between Bouguer disturbance and filtered topography over the South Atlantic.

- a) The variation in continental angular coefficient*
- b) The variation in oceanic angular coefficient*
- c) The variation in linear coefficient*
- d) The residual gravity field*
- e) The root mean square error*

Figure 7 – The differences between results from a two-stage robust regression and results from a singular regression across the South Atlantic.

- a) Differences in continental angular coefficient values*
- b) Differences in oceanic angular coefficient values*
- c) Differences in linear coefficient values*
- d) Differences in residual gravity values*
- e) Differences in RMS values*

Figure 8 – The differences between results from a two-stage robust regression and results from a standard two-stage regression across the South Atlantic.

- a) Differences in continental angular coefficient values*
- b) Differences in oceanic angular coefficient values*
- c) Differences in linear coefficient values*
- d) Differences in residual gravity values*
- e) Differences in RMS values*

List of Equations

Equation 1 – The continental crustal root equation.

Equation 2 – The oceanic crustal anti-root equation.

Equation 3 – The standard Bouguer plate approximation.

Equation 4 – The continental Bouguer disturbance.

Equation 5 – The oceanic Bouguer disturbance.

Equation 6 – The continental angular coefficient.

Equation 7 – The oceanic angular coefficient.

Equation 8 – The standard least-squares solution.

Equation 9 – The residual equation.

Equation 10 – The iteratively re-weighted least-squares solution.

Equation 11 – The root mean square equation (RMS).

Abstract

Isostatic response mechanisms provide an efficient means of decomposing gravity disturbances by modelling and removing the effects of compensating density contrasts situated at the crust/mantle interface. Here, the known method of separating the effects of an undulating Moho from anomalous crustal signals is refined through implementation of two individual robust regressions for continental and oceanic areas. The focus of the regression analysis is centred on the South Atlantic, including the African and South American continents. An iteratively re-weighted least squares approach was implemented whereby regression coefficients, residual values and data misfit estimates were reported from a best-fit predicted model of the linear relationship between filtered topography and the Bouguer anomaly. Continental regression coefficients exhibit erratic values and large degrees of error. However, stable coefficients with low misfit are returned in oceanic regions, where analysis of coefficients is identified as a promising tool for distinguishing between crustal structures. The residual gravity field is obtained through subtraction of the average regression relation. This demonstrates a capable ability to highlight areas of tectonic or volcanic activity, as well as locating large-scale crustal structures – such as the Walvis Ridge and the Rio Grande Rise.

1. Introduction

Increased availability of global gravity data has allowed for large advances in the use of gravimetry as a tool of investigation in areas of geological significance. In order to isolate the signal produced by these regions of interest, the measured gravity reading must first be decomposed into its various components. The Earth's gravity field varies with topography, latitude, and density heterogeneities within the crust. It is a combination of all the masses on the Earth and the perceived centrifugal acceleration due to the Earth's spin; a crucial part of gravity data processing is correcting for these known effects (Mussett et al., 2019). The centrifugal acceleration and the variations at differing latitudes due to the Earth's elliptical shape are removed through the normal gravity correction. The effect of the known topographic masses is removed through the Bouguer correction. This leaves irregularities in the crust-mantle interface, known as the Moho, and density anomalies within the crust. If the local crustal anomalies are to be analysed, the effect of the long-wavelength regional signal caused by the undulating Moho must first be removed.

One well-known method for accomplishing this is to assume that the Moho depth variations are due to isostatic compensation. A commonly used model is the Airy hypothesis of isostasy - this states that topographic loads are balanced by variations in crustal thickness, while assuming a uniform crustal density (Fowler, 2006). Mass excess, such as topography above sea level, is supported by a thickening of the crust. Conversely, mass deficit, such as an ocean basin, is supported by a thinning of the crust. When following Airy's theory, the relationship between topography and the gravitational effects of the isostatic Moho are shown to be linear. However, this is only true provided the wavelengths of topography are large enough. At short wavelengths the crustal loads are compensated through a lithospheric flexure response (Watts, 2001). Airy isostasy can be seen as a very long-wavelength approximation for the flexure theory, an increasing size of wavelength results in the isostatic compensation tending towards the Airy model. Topographic filtering is therefore necessary in order to validate the use of this hypothesis. Once this filtering has been applied, the gravity signal attributed to the Moho can be corrected for by fitting a linear equation to the observed data. The line of best fit is representative of the effect of the Moho and the deviation of data points from this general trend is characteristic of density heterogeneities within the crust. By subtracting the average regression relation from the corrected gravity field, the Moho signal is removed (Mussett et al., 2019). The remaining signal constitutes the residual gravity field, this is composed of gravity anomalies that are not correlated with isostatic compensation.

Using this method of regression as a means of separating crustal gravity signals from the Moho contribution has been successfully demonstrated in Africa (Braitenberg, 2015) and the South Atlantic

(Pivetta and Braitenberg, 2020). Before any analysis was performed within these two studies, a final topographic reduction was completed in order to make calculations transparent to both continental and oceanic crust. When performing a singular regression across a study area of both crustal compositions, a shift in the slope of the regression line occurs as the crustal type changes. This is due to a variation in the angular coefficient between the crustal types when a linear equation is applied to the gravity/topography relationship. To account for this, a manipulation of variables is performed, whereby an approximation of continental and oceanic crust density is used to construct an equivalent topography relating to both crust varieties (Braitenberg, 2015). This flattens the curve allowing for a single regression to be performed by making the angular coefficient uniform across the whole dataset. Once all the reductions were finalised, the linear relationship between filtered topography and corrected gravity could be used to distinguish between crustal sources; these isolated signals were then correlated with known geological structures. However, despite previous successes in applying this regression analysis to identify and study crustal anomalies, performing one singular regression relies on assumptions on the values of standard continental and oceanic crust densities. To achieve the full isostatic gravity correction without these assumptions two separate regressions are necessary – one for continental crust and one for oceanic crust.

In this study, the method for removing the effects of an isostatic Moho will be refined. Instead of performing a singular least-squares regression, two robust regressions are applied for continental and oceanic areas. This method is then considered in small windows across the full area of study, with the aim of further enhancing local anomaly signals. The chosen region of investigation is the South Atlantic and confining continents for the purpose of drawing comparisons with previous studies (Pivetta and Braitenberg, 2020). Analysis of the calculated regression coefficients is undertaken in an attempt to identify and distinguish between crustal structures, as well as investigation into the isostatic state of each region through determination of the mean square error. With the aim of validating refinements made to the pre-existing method, two further sets of results are acquired - one from a singular regression and one from a standard two-stage regression. Differences between these results are evaluated, and conclusions on the use of the robust model are presented.

2. Theoretical Background

Understanding of the key concepts behind the regression analysis is fundamental for validation of this method as a tool to remove the long-wavelength Moho contribution. Here, the derivation of the crustal root and anti-root equations following Airy's isostatic theory are illustrated, as well as the application of these equations to a standard Bouguer anomaly.

2.1 - Airy Isostasy

The Airy hypothesis of isostasy states that isostatic compensation is achieved by variations in crustal thickness (Fowler, 2006). A topographic load is supported by a root, whereas an oceanic basin is supported by an anti-root (Fig.1). The basis of the model follows the principle of hydrostatic equilibrium (Turcotte and Schubert, 1982) whereby the hydrostatic pressure is equal at every point at the same elevation. Using this principle, the thicknesses of the isostatic roots can be calculated by taking two arbitrary points at the depth of isostatic compensation and equating the lithospheric columns overlaying these positions. A derivation of the root thickness equations - aided by an illustration of Airy isostasy as shown by Figure 1 - is displayed below:

The hydrostatic equation relating pressure ' p ' to density ' ρ ', depth ' h ' and gravitational acceleration ' g '

$$p = \rho gh$$

Equating the pressures

$$\rho_1 gh_1 = \rho_2 gh_2$$

Applying this to the lithospheric structure shown in figure one

$$(t_1 + h + r_c)\rho_c = h\rho_c + r_c\rho_m$$

Hence, for a topographic load the crustal root equation is

$$r_c = \frac{\rho_c}{\rho_m - \rho_c} t_1 \quad (1)$$

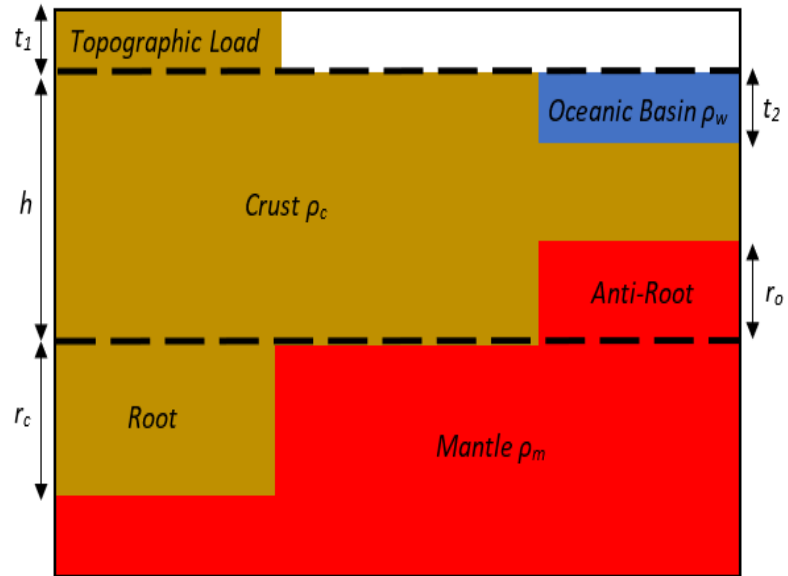


Figure 1 - An illustration of Airy isostatic compensation. Where t_1 represents the height of continental topography, t_2 the depth of the oceanic basin, h the reference Moho depth, r_c the thickness of a root, r_o the thickness of an anti-root and ρ_c , ρ_m and ρ_w the densities of crust, mantle and ocean water respectively.

Similarly, for an oceanic basin

$$h\rho_c = t_2\rho_w + r_o\rho_m + (h - t_2 - r_o)\rho_c$$

Therefore, the anti-root equation is given by
$$r_o = \frac{\rho_c - \rho_w}{\rho_m - \rho_c} t_2 \quad (2)$$

2.2 - Gravity/Isostasy Relationship

Once all reductions to gravity data have been made, the remaining signal is attributed to the undulating Moho and density irregularities in the crust (Fig.2). The fluctuating shape of the Moho is due to the compensation of topographic masses (Hofmann-Wellenhof and Moritz, 2006); adhering to Airy's theory, this compensation is fulfilled by crustal roots. Two varying equations relating topography and the thickness of the roots have been given following the derivation illustrated in Section 2.1. Utilising these relationships, the gravitational effect of the isostatic roots can be determined. This can be done through a simple Bouguer plate approximation – the standard equation is given as follows:

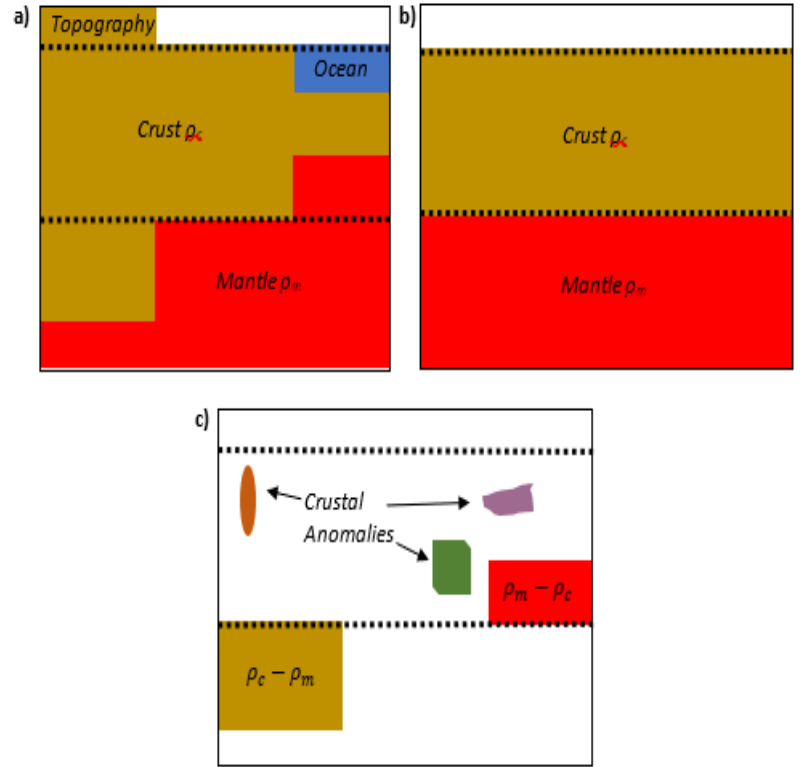


Figure 2 - An illustration of the effect of gravity data reductions. a) The real Earth pre-correction b) The normal Earth c) The remaining gravity disturbance after the removal of the effect of the normal Earth, and after topographic corrections. This signal contains the gravity signal from the roots/anti-roots attributed to an isostatic Moho, and any density anomalies in the crust.

$$g_{bg} = 2\pi G\rho t \quad (3)$$

in which G represents the gravitational constant and g_{bg} is the gravitational effect of a root with a thickness t and density ρ .

After the normal gravity reduction (Section 3.2) has been applied, the layered nature of the Earth is removed from the signal. In relation to isostatic roots, this results in varying density contrasts. This is because the normal Earth has mantle where the real Earth has a crustal root, and crust where the

real Earth has an anti-root composed of mantle. A basic illustration of this is shown by Figure 2.

Hence, the Bouguer approximations for oceanic and continental roots become

$$g_{bgcont} = 2\pi G(\rho_c - \rho_m)r_c$$

$$g_{bgocean} = 2\pi G(\rho_m - \rho_c)r_o$$

where ρ_c and ρ_m denote crustal and mantle densities, and r_c and r_o represent the thickness of a root and anti-root respectively.

Substitution of the derived equations for r_c and r_o (Section 2.1) then leads to

$$g_{bgcont} = -2\pi G\rho_c t \quad (4)$$

$$g_{bgocean} = 2\pi G(\rho_w - \rho_c)t \quad (5)$$

in which ρ_w denotes the density of ocean water and t represents topographic values. Due to topography in an ocean basin being located below the reference level, the values are negative and there is a reversal in sign.

Through these equations, two linear relationships between topography and the gravitational effects of an isostatic Moho are acquired. Therefore, provided topographic and gravity data are obtainable, regression analysis can be performed, and the Moho contribution can be corrected for.

3. Methodology

In this section, the procedure employed in obtaining the gravity and topographic data for the South Atlantic is presented - as well as any necessary corrections made to the datasets. This is followed by a description of the chosen methods of investigation, and the application of these methods to the amended data values.

3.1 - Data Acquisition

Gravity data was acquired from the EIGEN-6C4 global gravity field model. This is a spherical harmonic expansion model incorporating a combination of satellite and terrestrial data up to a maximum degree and order 2190 (Förste et al., 2014); the amalgamation of satellite and surface data parts was achieved using a band-limited combination of normal equations. Topographic data was taken from the ETOPO1 global relief model – a model of the Earth’s surface that integrates land topography and bathymetry (Amante and Eakins, 2009). The data are available at the International Centre for Global Earth Models (ICGEM, Ince et al., 2019) where grids for both these datasets were generated.

3.2 - Data Reduction

As is the case with many geophysical techniques, a prerequisite of investigating gravimetry measurements is the processing and filtering of the data. The removal of all the known effects from the gravity observations is necessary if anomalous crustal signals are to be analysed.

The first reduction applied is the removal of the gravity effects of an ellipsoidal reference Earth; this is referred to as the normal gravity correction. The elliptical shape of the earth causes the gravitational acceleration to vary due to the $\frac{1}{r^2}$ proportionality. In addition to shape, gravity differences are caused by the rotation of the Earth due to the effects of the centrifugal force. Subtracting normal gravity from the observed gravity field accounts for both the layered nature and rotation effect of the Earth. The difference between observed gravity and normal gravity is known as the gravity disturbance. Calculation of the normal gravity is performed using the closed-form solution (Li and Gotze, 2001); this allows for the magnitude of the gradient of the gravity potential generated by the ellipsoid to be computed at any height and latitude (Uieda, 2020), removing the need for the free-air approximation. In this study, the reference ellipsoid used is the WGS84 ellipsoid (Hofmann-Wellenhof and Moritz, 2006).

After the removal of normal gravity, the remaining disturbance consists of the following: topography, the residual effect of the oceans, crustal anomalies, and the isostatic Moho contribution. The oceanic residual effects are due to an overcorrection when subtracting normal gravity from the observed field; ellipsoid crust has been removed where the real Earth has ocean water (Uieda et al., 2020). Hence, the next reduction applied aims to correct for these residual bathymetry effects and for the effects of the topographic masses. Assuming default densities for the crust and ocean water (2670 kgm^{-3} and 1040 kgm^{-3} respectively), this was achieved through a simple Bouguer plate approximation.

Equation 3 was used for continental areas and Equation 5 for oceanic. Here, the Bouguer correction requires a “thickness” t of slab rather than height. Thickness values can only be positive. Therefore in reference to the approximation for the oceans, the absolute value of bathymetry needs to be taken. A comparison between the raw gravity anomaly and the final topography-free gravity disturbance is illustrated by Figure 3a and 3b respectively.

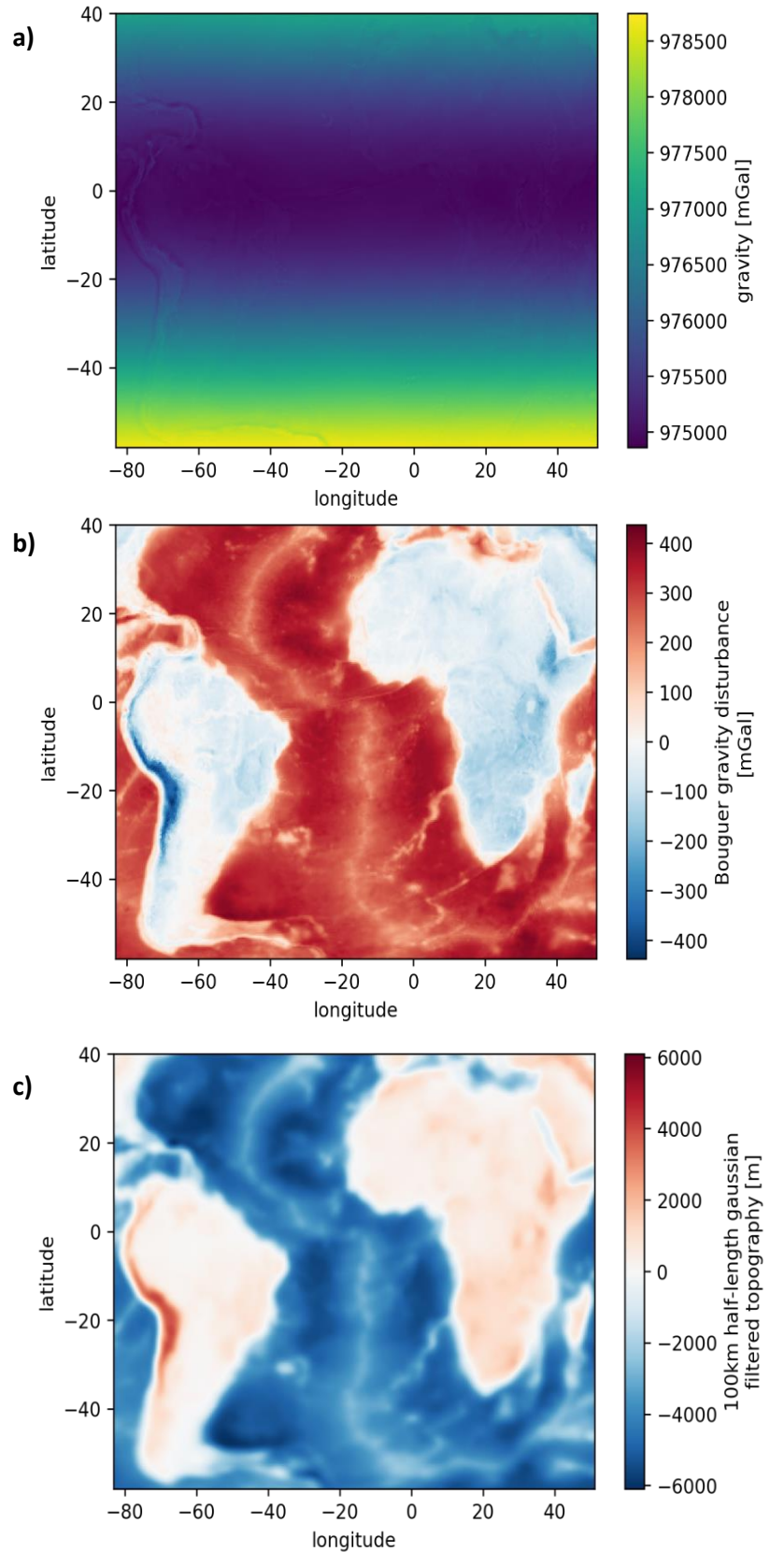


Figure 3 - a) Raw gravity data over the South Atlantic, acquired from the EIGEN-6C4 model b) The full reduced Bouguer gravity disturbance, after normal gravity and topographic corrections are applied. c) 100km half-length Gaussian filtered topographic profile, acquired from the ETOPO1 global relief model.

Lithospheric flexure theory predicts that Moho compensation only tends towards the Airy mechanism given the wavelengths of topography are large enough (Pivetta et al., 2019). Therefore, in order to validate the use of the Airy model of isostasy, filtering of the topographic data is required – this was done using a Gaussian filter of 100km half length. The filtered topographic profile can be seen in Figure 3c.

3.3 - Regression Analysis

Once all known effects of gravity have been corrected for, the remaining topography-free gravity disturbance can be decomposed into sources attributable to crustal anomalies - provided these signals are first separated from the effect of the undulating Moho. This separation can be achieved by performing a least-squares regression.

The least-squares method of regression fits a linear equation to observed data by minimizing the sum of the squared deviations between the data and best-fit line. Implementing this method, a linear regression line can be used to model the relationship between filtered topography and the gravitational effects of an isostatic Moho. Here, the average regression relation is representative of the Moho contribution. Subtracting this relation from the corrected gravity disturbance removes the Moho signal. What remains is a residual gravity field characteristic of crustal anomalies.

The linear relationships between filtered topography and the isostatic Moho for both continental and oceanic areas are illustrated by Equations 6 and 7. These equations can be written in the form:

$$y_i = \alpha_i t_i + \beta_i$$

in which the topography-free gravity disturbance is defined by the observed data y_i , filtered topography is denoted t_i , and α_i and β_i represent the angular and linear regression coefficients respectively.

With respect to these relationships,

$$\alpha = -2\pi G\rho_c \text{ for continental crust} \quad (6)$$

whereas

$$\alpha = 2\pi G(\rho_w - \rho_c) \text{ for oceanic crust.} \quad (7)$$

As a result of the varying angular coefficients, areas of both crustal compositions will observe differing slopes of regression when fitting a linear equation to the data. Due to this, two separate least-squares regressions need to be performed in these regions.

The standard least squares solution for a linear equation is:

$$p_i = [A^T A]^{-1} A^T y_i \quad (8)$$

in which p_i denotes the model parameters, A the sensitivity matrix, and y_i the observed data values.

Three model parameters are returned from the least-squares regressions performed on the Bouguer anomaly: the continental angular coefficient α_c , the oceanic angular coefficient α_o and the linear coefficient β . Due to the proportionality with crustal densities, variation in angular coefficients indicate changes in crustal composition. This can be used as a means to distinguish between crustal structures. With respect to the linear coefficient it is predicted that following an isostatic model a zero value should be observed (Pivetta and Braitenberg, 2019) – however, this is often not the case. There is still large debate as to what the occurrence of a non-zero linear coefficient signifies, therefore for the purpose of this study focus will not be placed on this.

The residual gravity field is obtained once the regression line is removed from the observed data. The deviation of these residual data points from the general trend indicates crustal structures that do not observe a pure isostatic response - something that is typical of crustal density heterogeneities. Attributing the local crustal anomalies to known geological features is then plausible; this is completed through analysis into the varying coefficients, supported by examination of the remaining residual sources.

3.4 - Robust Fit

One disadvantage with the least-squares method of regression is the sensitivity of the model to outliers. Outlier bias can significantly impact the results of an analysis by skewing the slope of the regression line. The effect of these outliers needs to be removed or negated before any definitive analysis can take place. However, complete removal of the outliers is not a pragmatic approach. This would require finding all outliers from the datasets through a manual process, and due to the sheer quantity of data when dealing with topographic and gravimetry values across a continent-wide scale, this process would be neither realistic nor time efficient. Instead, the effects of any outliers are negated by applying a robust fit to the data through an iteratively re-weighted least squares approach.

The iteratively re-weighted least squares method works by implementing a weighted matrix into the standard least-squares solution. Once a preliminary least-squares regression has been completed, predicted data values are obtained, and these can be subtracted from the observed data in order to acquire values for the residuals. The equation below illustrates this:

$$r_i = y_i - \hat{y}_i \quad (9)$$

where r_i denotes the residuals, and \hat{y}_i the predicted data.

These residuals are then used to construct a weighted matrix W , whereby the main diagonal is filled with values of $\frac{1}{r_i^2}$ up to an n_{th} value of r . The remainder of the matrix consists of zero values.

Applying this weighted matrix to the normal least squares equation allows for recalculation of the model parameters and residuals -

the reweighted least-squares

solution is as follows:

$$p_i = [A^T W A]^{-1} A^T W y_i \quad (10)$$

For residuals with particularly large values (e.g. outliers) the weight of this data will be extremely small.

The smaller the weight, the less impact these points have when the re-weighted regression relation is calculated. This shifts the regression line away from the outliers. If the line moves away from the outlier, the residual value

increases, therefore reducing the size of the weight. These new weights are then re-iterated back into the least squares solution, and the regression line shifts once again. This process can be repeated a chosen finite amount of times resulting in the regression line progressively moving away from the outliers, and therefore negating their effects on the final fitted model. A simplified application of the re-weighted least squares method to a generic dataset is illustrated by Figure 4.

3.5 - Root Mean Square

The root mean square (RMS) is a measure of accuracy, it is used to observe the differences between actual data and the values predicted by a fitted model. This gives an estimate of how well the data fits the regression, or the level of misfit of the data. Root mean square can be estimated using the residuals:

$$RMS = \sqrt{\frac{1}{N} \sum_{i=1}^N (y_i - \hat{y}_i)^2} = \sqrt{\frac{1}{N} \sum_{i=1}^N (r_i)^2} \quad (11)$$

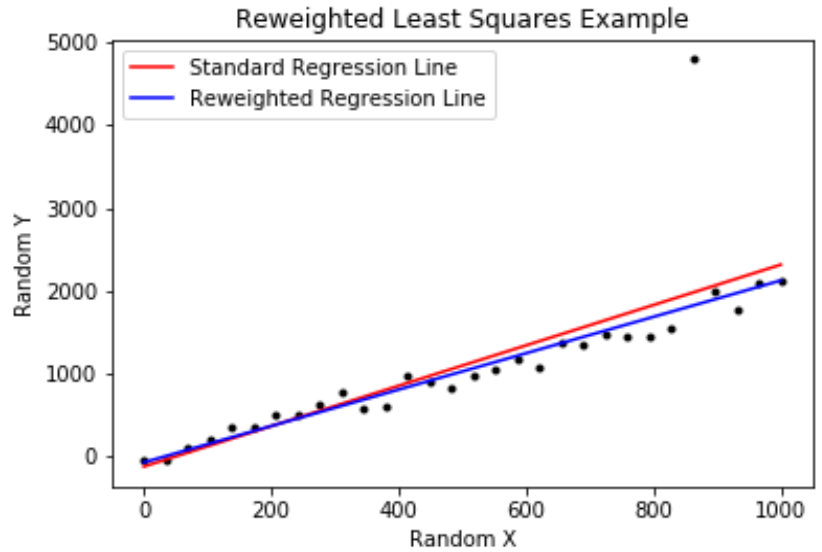


Figure 4 - An example of applying a robust fit to an arbitrary dataset through the method of iteratively re-weighted least squares. Here, the red regression line represents a standard least squares solution, whereas the blue regression line indicates the re-weighted least squares solution. Implementing the re-weighted approach progressively shifts the regression line away from the effect of outliers.

Observing how RMS values vary across the study area can give an indication of the isostatic state of the lithosphere and therefore demonstrates how well each region follows the Airy mechanism. Where the fit to the regression line is poor, large RMS values will be returned. This can be used to highlight areas that do not exhibit an isostatic response – something synonymous with crustal density anomalies or regions of high tectonic activity.

3.6 - Application in Windows

In order to gain an improved understanding of how the lithospheric structure varies by region the robust regression analysis was applied in multiple batches across the entire dataset. Considering the regression in small windows of analysis allows for better local estimates to be obtained, and therefore emphasizes the signal from any heterogenic crustal sources. When selecting the defining parameters, the window size should allow increased sensitivity of the regression coefficients to local variations while simultaneously remaining large enough to detect an isostatic response. The regression analysis was applied in 3° by 3° windows for this study, enabling comparisons to be drawn with previous research (Pivetta and Braitenberg, 2020).

4. Results

The best-fitting regression relation for the final Bouguer disturbance and filtered topography across the South Atlantic is illustrated by Figure 5. As expected, the regression line shows an anti-correlated relationship between the two datasets. This is due to the negative value of angular coefficient when modelling an isostatic response (refer to Equations 6 and 7). The observed regression line over the oceanic areas is less steep than that of continental regions. The gradient of these lines is

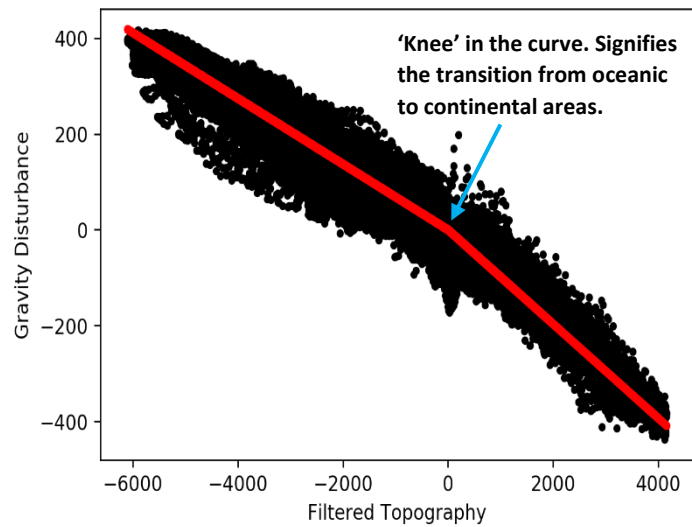


Figure 5- The approximated best-fit least squares solution to the Bouguer disturbance and filtered topography data across the South Atlantic. The predicted regression line is indicated in red, the deviation of data points from this line reflect anomalies uncorrelated with topography, and therefore also isostasy.

most likely influenced by the isostatic compensation depth. For areas of high topographic relief, the model predicts a large negative Bouguer disturbance; for areas of deep bathymetry a positive anomaly is expected. This is consistent with the isostatic mechanism as crustal roots will cause a mass deficiency in relation to the denser mantle, whereas anti-roots will result in a mass excess. All the data points that fall outside the regression line represent residual signals; these reflect inhomogeneities not correlated to isostasy. The results observed in this section provide figures of the varying regression coefficients, residual signals, and data misfit over the South Atlantic calculated through a two-stage robust regression. A one-stage regression determined implementing equivalent topography (Braitenberg, 2015) and a non-robust two-stage regression were also performed. The results from these alternative regressions were then subtracted from the robust method with the aim of highlighting any significant differences.

4.1 - Regression Coefficients

Figure 6a, 6b, and 6c detail the spatial distribution of the angular continental, angular oceanic and linear regression coefficients in 3° by 3° windows over the South Atlantic. The values of the angular coefficient are predominantly negative across both continental and oceanic crust as predicted by the regression, however over the continents the values show much greater variability (Fig.6a). In central South America, the observed slope coefficient varies from positive values of approximately

4. Results

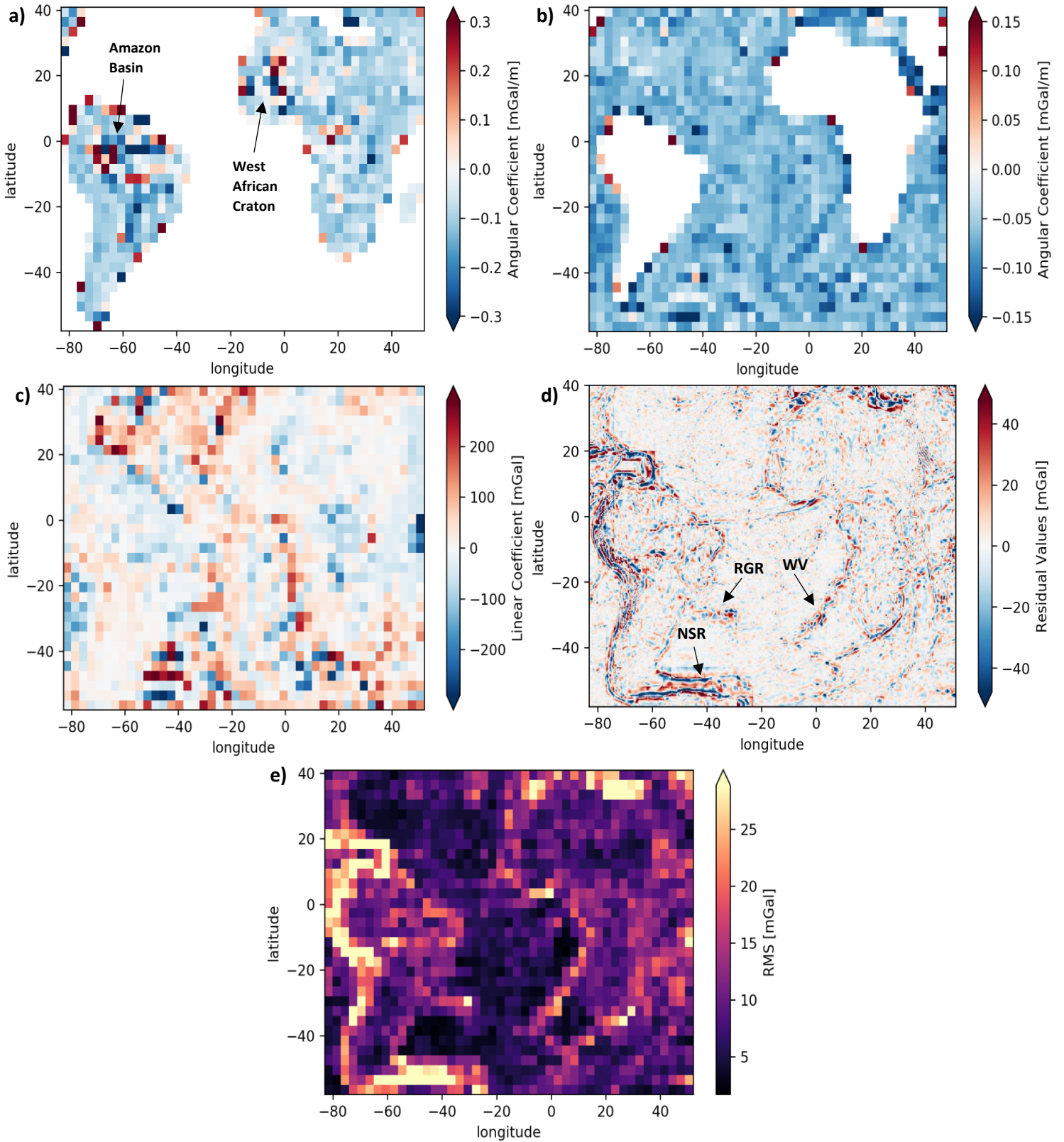


Figure 6- Results for the regression coefficient, residual gravity, and root mean square error values across the South Atlantic. a) The variation in the angular coefficient over continental regions. b) The variation in the angular coefficient over oceanic regions. c) The variation in the linear coefficient. d) Residual gravity field. e) Root mean square error. Regressions performed in 3° windows of latitude and longitude. Significant geological structures marked: Amazon Craton, West African Craton, North Scotia Ridge (NSR), Walvis Ridge (WV), Rio Grande Rise (RGR). The angular coefficients are plotted separately for continental and oceanic crust due to overlapping results in windows where both crustal types occur.

0.3 mGal/m to strong negatives of approximately -0.3 mGal/m; a cluster of varying coefficients also occurs in Western Africa. These regions contain the Amazonian Craton and the West African Craton, respectively. In comparison, the oceanic areas observe a relatively homogenous angular coefficient, varying by around 0.15 mGal/m, which indicates that areas of older continental lithosphere have a much more heterogenous lithospheric structure than the newer oceanic crust – such as the regions surrounding the Mid Atlantic Ridge. Positive angular coefficients are observed relatively frequently on the edge of the continents, where crustal type transitions from oceanic to continental.

With respect to the linear coefficients, the variation in the values across the full study area are much more erratic (Fig.6c). Ribbons of high positive values are however observed along the continental edges, distinguishing the change from oceanic to continental crust. In general, the values of the linear intercept are much greater in oceanic areas. Moving towards the centre of continental areas, the values tend towards zero or fall to low negatives. This supports the results observed from the angular coefficient map, whereby the varying values across crustal types suggest clear contrasts in lithospheric structure.

4.2- Residual Values

The residual gravity field (calculated according to Equation 9) is reported by Figure 6d - this contains the remaining gravity signal observed by data points that deviate from the predicted regional trend. Here, the continents show much larger anomalous values than the oceanic areas. The most prominent anomalies tend to occur at plate boundaries: the Caribbean Arc at north of South America, the Peru/Chile trench on the western Coast, and the North Scotia Ridge situated in the south of the Continent. Significant residuals are also observed in a large fault zone situated in northern Africa and by two ocean ridges occurring in the South Atlantic– the Rio Grande Rise (RGR) and the Walvis Ridge (WV). The residuals at each of these locations illustrate typical dipolar anomalies, whereby couples of positive and negative values highlight each region. As with the regression coefficients, the residual map highlights the boundaries between oceanic and continental areas, indicating the change in crustal structure. Isolated residuals are observed towards the centre of the continents, with emphasis on prominent dipolar signals occurring in central South America.

4.3 - Data Misfit

The error in the observed results was measured by determining the root mean square (RMS) for each data value (Equation 11). By computing the RMS, a measure of how well the data fit the regression model is quantified and therefore an estimate to the accuracy of the spatial analysis is provided. A visualisation of the varying data misfit across the South Atlantic is illustrated in Figure

6e. The general trend shows that the predicted data over the continents is more erroneous than that of the oceans. The low values of RMS reported throughout the oceanic areas suggest that the topography in these regions generally exhibits an isostatic response. As expected, the highest RMS values occur in areas where high levels of tectonic activity are exhibited – such as plate margins and regions of hotspot volcanism (e.g. The Rio Grande Rise and Walvis Ridge).

4.4 - Differences between one-stage and robust two-stage regression results

Regression coefficients, residuals and error values were similarly acquired through a one-stage regression. Subtracting these results from the data provided by the robust method led to the profiles illustrated by Figure 7. A clear trend can be seen in all these maps whereby the continental borders are heavily outlined by the remnant values. In Figure 7a and 7b the difference in angular coefficients observed are mostly positive values, with all large differences occurring on the continent edges. Towards the centre of the continents the regressions seem to return equal results, and in the oceanic areas a trend of low uniform positive differences is observed. The difference between the linear coefficients (Fig.7c) highlights narrow areas of high negative and positive values surrounding the continents. Once again, the values returned from each regression seem to be most similar within the continental areas. Oceanic areas in contrast display very inconsistent values. Within the residual profile (Fig.7d), the continental margins display a pattern showing a positive value flanked by negative values. This pattern can be clearly seen around the perimeter of Africa and northernmost South America. However in southern South America the reverse appears to be the case. The difference in RMS values (Fig.7e) mirror the residual map in that the greatest differences all occur around the margins of the continents.

4.5 - Differences between standard two-stage and robust two-stage regression results

After observing the differences between a one-stage and two-stage regression, the same technique was applied to evaluate the changes in results between a standard two-stage and robust-two stage regression. These differences are reported by Figure 8. Here, the differences in angular coefficients (Fig.8a and Fig.8b) are low and uniform over regions containing purely oceanic crust, whereas continental windows show much higher variability - the highest differences tend to occur on the continental borders. Two significant values can be seen on the eastern coast Africa at an equatorial latitude, whereby the same windows produce positive differences in angular coefficient values in figure 8a and negative differences in oceanic angular coefficient values in Figure 8b. The differences in linear coefficients (Fig.7c) are irregular, however in general higher changes can be observed in the oceans. In Figure 7d, the biggest differences in residual values seem to occur at plate margins, such as the subduction zone in western South America and the North Scotia ridge in southern South

4. Results

America. One prominent point is seen on the African coast at approximately 0° latitude and longitude. This region indicates sloping positive to negative values in a northwards direction. The RMS values (Fig.7e) show the most difference in regions of tectonic activity, however in general all RMS differences are very low, with a maximum value of around 0.25 mGal.

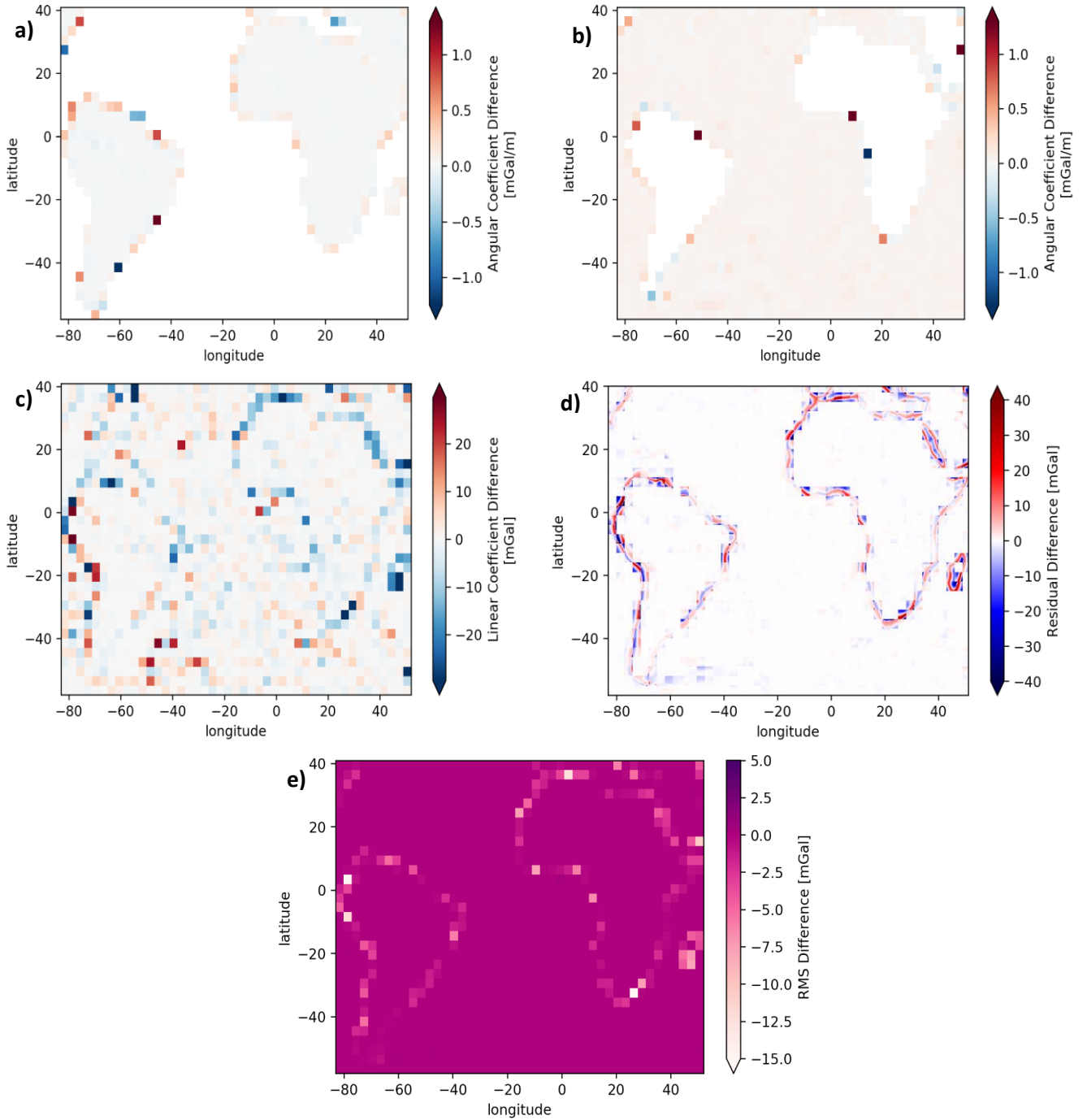


Figure 7 – The differences between results from a two-stage robust regression and results from a singular regression across the South Atlantic. a) The continental angular coefficient values. b) The oceanic angular coefficient values c) The linear coefficient values. d) The residual values. e) The RMS values. Regressions performed in 3° by 3° windows of longitude and latitude.

4. Results

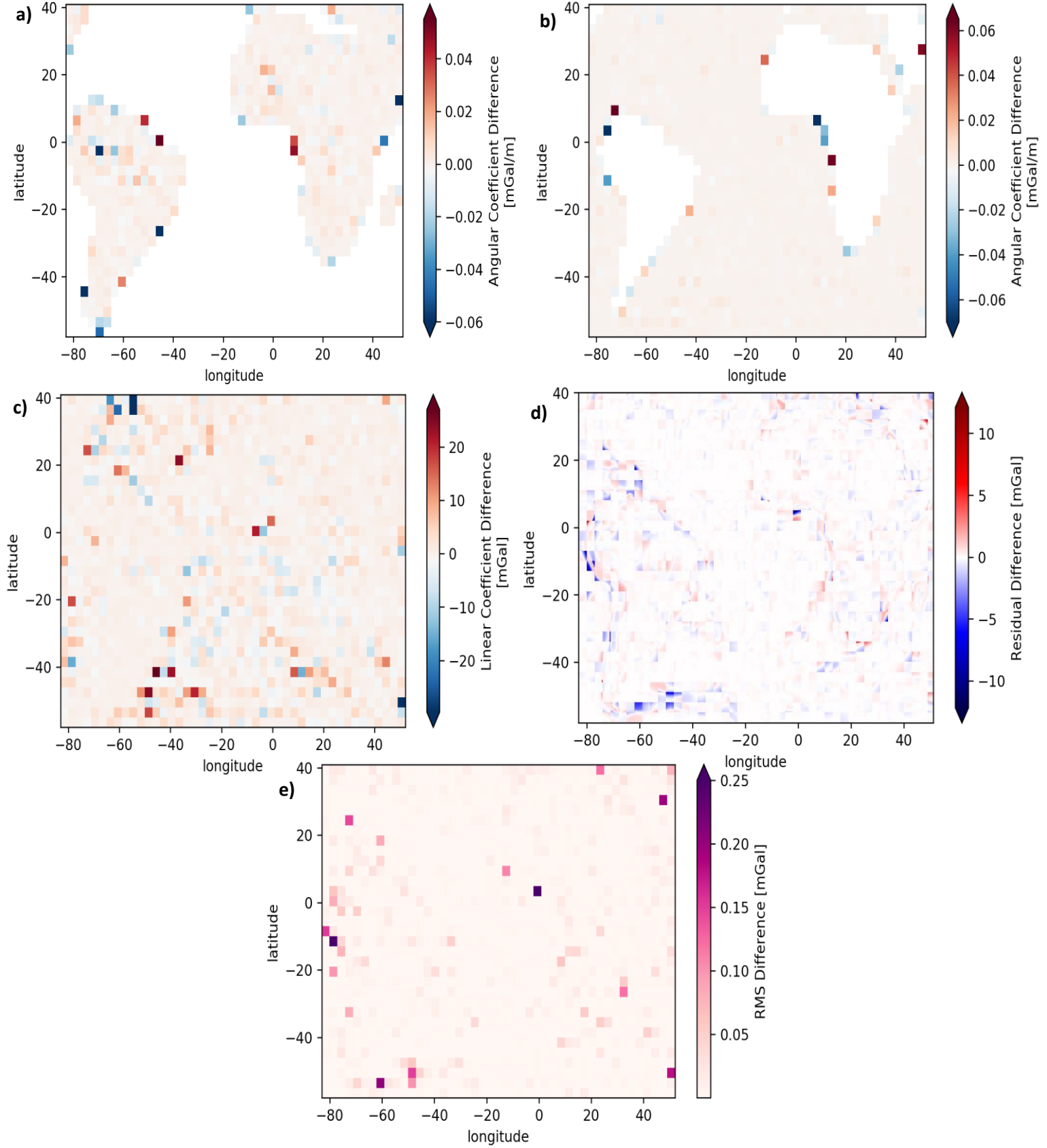


Figure 8 – The differences between results from a robust two-stage regression and results from a standard two-stage regression across the South Atlantic. a) The continental angular coefficient values. b) The oceanic angular coefficient values c) The linear coefficient values. d) The residual values. e) The RMS values. Regressions performed in 3° by 3° windows of longitude and latitude.

5. Discussion

5.1 - Application of the regression analysis to the South Atlantic area

The regression analysis illustrated large variability of angular coefficients in continental areas with contrasting stable and uniform values reported in oceanic areas. The most prominent features on the angular coefficient maps (Fig.6a and Fig.6b) occur in the Amazon Basin and in the West African Craton – the erratic values reported by these regions can be attributed to their complex geological structures. For example, the Amazon Basin is situated within a Large Igneous Province (LIP) (Klein et al., 2012) containing multiple layers of high-density volcanic rocks. The regression model fitted assumes a one-layered, one-density isostatic response; in areas of heterogenous continental lithosphere tectonic processes have resulted in a crustal structure with a variety of compositions, the model chosen does not account for this. In contrast, values from the oceanic areas seem to report a good fit to the model. The Mid-Atlantic Ridge (MAR) reports stable negative values for the angular coefficient, as predicted by an isostatic mechanism (Equation 6 and 7). Here, the MAR is compensated through a Pratt response, whereby decompression and heat-flow cause lateral variations in crustal densities (Fowler, 2004). The chaotic linear coefficient values displayed by the oceans (Fig.6c) may be attributed to large amounts of sediment cover resulting in differences in the model. Non-zero linear coefficients are also expected in regions where flat topography spans across large distances (Pivetta and Braitenberg, 2020). This feature is characteristic in oceanic areas.

The residual and RMS maps (Fig.6d and Fig.6e) highlight plate boundaries and continental margins. The greatest values observed can be seen in areas of significant tectonic activity where the fit to an isostatic model is poor. On the western coast of South America, the large RMS and residual signal is attributed to the convergent margin between the Nazca and South American plates. This collision results in the large subduction zone marked by the Peru/Chile trench and the Andean orogeny. The dipolar residual signals observed are most likely caused by this subduction, whereby the depression of the trench and flexural bulge of the lithosphere cause differing anomalies. In addition to this, the sharp topographic relief of the Andes exhibits a strong residual signal. Steep topography breaks down the Bouguer approximation and the Airy isostatic model because an abrupt change in topographic load causes the crust to bend – a flexure response. Other prominent anomalous values indicate the existence of a significant fault zone in northern Africa and large variations of crustal thickness occurring at the North Scotia Ridge in southernmost South America (Cunningham, 1998).

Smaller scale lithospheric structures can also be identified from Figure 6d and 6e. The clearest of these are the Rio Grande Rise, the Walvis Ridge and the Amazon Basin – all examples of magmatic provinces. This suggests that calculating residual and RMS values may be a useful tool in identifying

areas of past volcanic activity. Moving to the east of the Amazon Basin, residual values are observed on the Brazilian coast. One potential cause of these is the mouth of the Amazon River, here large deposition of sediment will occur creating layers of extra mass. As previously stated, the model used in this analysis assumes a one-layer crust, therefore these added layers of sediments are not accounted for. Further east still, a trace of residuals can be seen running from the Brazilian coastline to the African coast, this ribbon of values highlights a large fracture zone cutting the South Atlantic.

5.2 - Comparisons between varying regression methods

Figure 7 illustrates the differences between results obtained from a robust two-stage regression and results from a singular regression. As expected, the greatest differences all occur in areas where the crustal type transitions from continental to oceanic crust, this feature is robust in all five figures. In these continental margins, the windows show predominantly negative RMS difference values, suggesting that the data misfit in these areas is greater in the singular regression, and therefore validating the use of a two-stage method. The residual differences (Fig.7d) show a curious trend of reversing positive and negative values flanking the continents. The nature of this trend is yet unknown and therefore should be a subject of future investigation.

Comparisons between the use of a robust two-stage and standard two-stage regression are illustrated by Figure 8. With the exception of the linear coefficient (Fig.8c), these results indicate that the greatest differences occur in the continental regions. This is most likely due to the heterogeneous nature of old continental lithosphere in comparison to younger oceanic crust, resulting in the data in these regions being more erratically spread around the regression line. As highlighted in the results, two windows on the east coast of Africa show positive differences in continental angular coefficients (Fig.8a) but negative differences in oceanic angular coefficients (Fig.8b). The RMS on these values is small suggesting that there is a similar fit to the model with two different sets of results. This indicates that there may be non-uniqueness in the regression within the continental borders. Moving north of these windows, one region of prominent dipolar differences is reported in the residual map (Fig.8d). Here the differences slope from positive in the south to negative in the north, presumably caused by an anomalous crustal structure. Large differences are seen in the west and south of South America, the regions containing these values are situated on active plate margins, implying the robust fit may be more sensitive to tectonic activity.

5.3 - Limitations

Although the regression analysis successfully indicated crustal structures and density variations, limitations within the method are still apparent. Firstly, the topographic correction applied was a standard Bouguer correction (Equation 3 for continental regions and Equation 5 for oceanic regions). This correction assumes an infinite slab of uniform density and thickness; therefore it is only an approximation. This infinite plate approximation is adequate for areas of flat topography, however for areas where topography varies dramatically, such as the Andes, a full proper topographic reduction should be performed. This can be done through the implementation of tesseroids. Tesseroids are spherical prisms that perform forward modelling of gravitational fields in spherical coordinates (Uieda et al., 2016). With this model the topographic data can be discretized and therefore variations in topography can be fully corrected for. Furthermore, the regression model applied does not take dynamic topography into account. Dynamic topographic relief is generated by movement in the mantle rather than surface processes (Braun, 2010), it is not supported through isostatic compensation. An example of dynamic topography occurs in the Patagonia region at the southern end of South America (Guillaume et al., 2009). The regression analysis provides no correction for this, therefore dynamic topography signals are observed within the calculated residuals.

Other limitations come from assumptions within the model. The method applied only takes local isostasy into account, in general this is only true for very long wavelengths of topography. Filtering was applied in order to validate the local isostatic model; however this resulted in a trade-off, whereby signals resulting from small-scale crustal anomalies supported by a regional response would be removed. In addition to this, a one-layer, one-density crust is assumed – real lithospheric structure can be much more complex than this.

6. Summary

6.1 – Conclusion

The robust regression analysis between the Bouguer disturbance and filtered topography has proven to be an effective technique for distinguishing crustal type and identifying large-scale geological structures. It provides a tool for removing the long-wavelength, regional effects of an isostatic Moho, and therefore can be used to study the isostatic state of the lithosphere. Through application of localised windows, the Bouguer disturbance could be decomposed and attributed to differing crustal sources. Across the South Atlantic, geological provinces and areas of high tectonic activity or volcanism are marked: the Amazon Basin, the West African Craton, the North Scotia Ridge, the Rio Grande Rise, and the Walvis ridge. Analysis of the angular regression coefficient showed erratic values within older, heterogeneous continental crust, but mostly stable negative coefficients in younger oceanic crust. Comparing this with values of RMS show that the data misfit is significantly lower across oceans, which suggests changes in coefficient throughout oceanic areas are a reliable parameter in indicating variations in crustal composition. The residual gravity field and RMS map demonstrate an apt ability to identify regions of tectonic or volcanic activity, as well as isolated crustal anomalies not correlated to isostasy.

Comparisons between a singular and two-stage regression indicate large differences in results within regions composed of both continental and oceanic crust - most prominently continental margins. These differences indicate that the data misfit in windows of both crustal types is greater in the singular regression, most likely due to a larger amount of assumptions within this model. Furthermore, implementing a robust regression illustrated increased sensitivity in regions of tectonic activity, as well as further highlighting local variations in crustal compositions. These findings therefore validate the implementation of a new and refined regression technique.

6.2 - Future work

The analysis performed in this study was solely over the South Atlantic and the surrounding continents. However, the method implemented is analogous to all areas therefore could be used as a means to investigate gravity fields globally, or even to study celestial structures. In respect to the results from this analysis, comparing the known regression method with the refined technique illustrated a fluctuating pattern of positive and negative residual differences flanking continental margins (Fig.7d). The cause of the dipolar trend is beyond the capabilities of this investigation and therefore further study into its nature is required. In addition to this, focus could be placed on regions containing isolated anomalous signals, such as those in central South America. By locating

these specific windows, a localised and concentrated regression can be performed and further interpretation of the source of these anomalies can be formed.

References

- Amante, C. and B.W. Eakins. (2009).** *ETOPO1 1 Arc-Minute Global Relief Model: Procedures, Data Sources and Analysis*. NOAA Technical Memorandum NESDIS NGDC-24. National Geophysical Data Center, NOAA. doi:10.7289/V5C8276M [15th April 2020].
- Braitenberg, C. (2015).** *Exploration of tectonic structures with GOCE in Africa and across-continentals*. *International Journal of Applied Earth Observation and Geoinformation*, 35, pp.88-95.
- Braun, J. (2010).** *The many surface expressions of mantle dynamics*. *Nature Geoscience*, 3(12), pp.825-833.
- Cunningham, Alexander P. (1998).** *Geophysical Investigations of the North Scotia Ridge*. University of London, PhD Thesis.
- Förste, Christoph; Bruinsma, Sean.L.; Abrikosov, Oleg; Lemoine, Jean-Michel; Marty, Jean Charles; Flechtner, Frank; Balmino, G.; Barthelmes, F.; Biancale, R. (2014).** *EIGEN-6C4 The latest combined global gravity field model including GOCE data up to degree and order 2190 of GFZ Potsdam and GRGS Toulouse*. GFZ Data Services. <http://doi.org/10.5880/icgem.2015.1>
- Fowler, C. (2006).** *The Solid Earth*. Cambridge, UK: Cambridge University Press, pp.202-204.
- Guillaume, B., Martinod, J., Husson, L., Roddaz, M. and Riquelme, R. (2009).** *Neogene uplift of central eastern Patagonia: Dynamic response to active spreading ridge subduction?*. *Tectonics*, 28(2), p.n/a-n/a.
- Hofmann-Wellenhof, B. and Moritz, H. (2006).** *Physical Geodesy*. Vienna: Springer-Verlag Wien, pp.83-90, 141.
- Ince, E. S., Barthelmes, F., Reißland, S., Elger, K., Förste, C., Flechtner, F., Schuh, H. (2019).** *ICGEM – 15 years of successful collection and distribution of global gravitational models, associated services and future plans*. - *Earth System Science Data*, 11, pp. 647-674, DOI: <http://doi.org/10.5194/essd-11-647-2019>.
- Li, X. and Götze, H. (2001).** *Ellipsoid, geoid, gravity, geodesy, and geophysics*. *GEOPHYSICS*, 66(6), pp.1660-1668.
- Mussett, A., Khan, M. and Button, S. (2019).** *Looking Into The Earth*. Cambridge: Cambridge University Press, pp.115-117,132.
- Pivetta, T. and Braitenberg, C. (2020).** *Sensitivity of gravity and topography regressions to earth and planetary structures*. *Tectonophysics*, 774, p.228299.
- Turcotte, D. and Schubert, G. (1982).** *Geodynamics*. New York: Wiley, p.397.
- Uieda, L. (2020).** *Boule: Reference Ellipsoids For Geodesy, Geophysics, And Coordinate Calculations*. [online] Zenodo. Available at: <<http://doi.org/10.5281/zenodo.3603997>> [Accessed 20th April 2020].
- Uieda, L., Barbosa, V. and Braitenberg, C. (2016).** *Tesseroids: Forward-modeling gravitational fields in spherical coordinates*. *GEOPHYSICS*, 81(5), pp.F41-F48.
- Uieda, L., Soler, S., Pesce, A., Oliveira Jr, V. and Shea, N. (2020).** *Harmonica: Forward Modeling, Inversion, And Processing Gravity And Magnetic Data*. [online] Zenodo. Available at: <<http://doi.org/10.5281/zenodo.3628742>> [Accessed 20 April 2020]

Watts, A. (2001). *Isostasy And Flexure Of The Lithosphere*. Cambridge: Cambridge University Press, Chapter 5.

